Am J Physiol Lung Cell Mol Physiol 287: L1303–L1313, 2004.
First published September 3, 2004; doi:10.1152/ajplung.00240.2004.

Tumor necrosis factor-α-induced TRPC1 expression amplifies store-operated Ca^{2+} influx and endothelial permeability

Biman C. Paria, Stephen M. Vogel, Gias U. Ahmmed, Setara Alamgir, Jennifer Shroff, Asrar B. Malik, and Chinnaswamy Tiruppathi

Department of Pharmacology, College of Medicine, University of Illinois at Chicago, Chicago, Illinois 60612

Submitted 28 June 2004; accepted in final form 29 August 2004

Paria, Biman C., Stephen M. Vogel, Gias U. Ahmmed, Setara Alamgir, Jennifer Shroff, Asrar B. Malik, and Chinnaswamy Tiruppathi. Tumor necrosis factor-α-induced TRPC1 expression amplifies store-operated Ca^{2+} influx and endothelial permeability. *Am J Physiol Lung Cell Mol Physiol* 287: L1303–L1313, 2004. First published September 3, 2004; doi:10.1152/ajplung.00240.2004.—We determined the effects of TNF-α on the expression of transient receptor potential channel (TRPC) homologues in human vascular endothelial cells and the consequences of TRPC expression on the endothelial permeability response. We observed that TNF-α exposure increased TRPC1 expression without significantly altering expression of other TRPC isoforms in human pulmonary artery endothelial cells (HPAEC). Because TRPC1 belongs to the store-operated cation channel family, we measured the Ca^{2+} store depletion-mediated Ca^{2+} influx in response to thrombin exposure. We observed that thrombin-induced Ca^{2+} influx in TNF-α-stimulated HPAEC was twofold greater than in control cells. To address the relationship between store-operated Ca^{2+} influx and TRPC1 expression, we overexpressed TRPC1 by three- to fourfold in the human dermal microvascular endothelial cell line (HMEC) using the TRPC1 cDNA. Thrombin-induced store Ca^{2+} depletion in these cells caused approximately twofold greater increase in Ca^{2+} influx than in control cells. Furthermore, the inositol 1,4,5-trisphosphate-sensitive store-operated cationic current was increased greater than twofold in TRPC1-transfected cells compared with control. To address the role of Ca^{2+} influx via TRPC1 in signaling endothelial permeability, we measured actin-stress fiber formation and transendothelial monolayer electrical resistance (TER) in the TRPC1 cDNA-transfected HMEC and TNF-α-challenged HPAEC. Both thrombin-induced actin-stress fiber formation and a decrease in TER were augmented in TRPC1-overexpressing HMEC compared with control cells. TNF-α-induced increased TRPC1 expression in HPAEC also resulted in marked endothelial barrier dysfunction in response to thrombin. These findings indicate the expression level of TRPC1 in endothelial cells is a critical determinant of Ca^{2+} influx and signaling of the increase in endothelial permeability.

tumor necrosis factor-α; store-operated calcium ion influx; transient receptor potential channel 1; endothelial barrier dysfunction

MICROVASCULAR ENDOTHELIAL cells regulate the vessel wall permeability of solutes, liquid, and macromolecules and produce numerous autocrine and paracrine factors, such as NO, that modulate the contractility of the underlying vascular smooth muscle (4, 5, 21). Endothelial cells thus contribute to the maintenance of vascular tone and essential barrier property of the vessel wall (4, 5, 19, 21). Proinflammatory mediators such as thrombin and histamine and reactive oxygen species can increase vascular permeability by activating Ca^{2+}-sensitive signaling pathways (35). In recent studies, we showed that Ca^{2+} entry through plasma membrane cation channels activated by Ca^{2+} store depletion is a critical determinant of increased endothelial permeability (30, 31, 33).

We have also shown that activation of endothelial cell surface protease-activated receptor-1 (PAR-1) by thrombin caused a rapid and transient increase in cytosolic Ca^{2+} concentration ($[Ca^{2+}]_i$) because of the release of stored Ca^{2+} and a subsequent Ca^{2+} entry triggered by store depletion (7, 20, 30). In endothelial cells, the plasma membrane cation channels known as store-operated cation channels (SOCs) mediate the entry of Ca^{2+} into the cell (2, 27, 32). Several studies have shown clearly influx of Ca^{2+} through SOCs in human vascular endothelial cells (1, 13, 25, 27, 33). Studies have also identified that the mammalian homologues of the transient receptor potential (TRP) gene family of channels function as SOCs (14, 18, 27, 29 33, 42). These TRP genes encode a superfamily of proteins with six transmembrane helixes that are divided into the following four subfamilies: TRPC (canonical or classical), TRPV (vaniloid receptor-related), TRPM (melastatin-related), and TRPP (PKD-type) (1, 24). Members of the TRPC subfamily contain 700–1,000 amino acids, and seven isoforms (TRPC1–7) are expressed in mammalian cells. Mammalian TRPCs are grouped into the following four subfamilies. *1*) One group consists of TRPC4 and TRPC5. Their activation is dependent on Ca^{2+} store depletion, and they have high Ca^{2+} selectivity, as assessed by their sensitivity to La^{3+} (13, 27). TRPC4 and TRPC5 are activated by G protein-coupled receptors and receptor tyrosine kinases coupled to phospholipase C. *2*) TRPC1 is closely related to TRPC4 and TRPC5; although it forms SOCs, it is a less selective Ca^{2+} channel. *3*) TRPC3, TRPC6, and TRPC7 form store-independent nonselective cation channels that may be activated by diacylglycerol (3, 24, 27); however, a store-dependent activation mechanism has been described for human TRPC3 (18). *4*) TRPC2 function is unclear, and it may function as a pseudogene in humans (24).

Primary endothelial cells in culture express TRPC1–TRPC6 to varying degrees (13, 14, 33). Mouse aortic and lung endothelial cells express TRPC1, TRPC3, TRPC4, and TRPC6, but TRPC4 expression is most pronounced in mouse endothelial cells (14, 33). Deletion of TRPC4 in mouse caused a marked impairment in store-operated Ca^{2+} current, and the Ca^{2+} store release activated Ca^{2+} influx in aortic and lung endothelial cells (14, 33). In TRPC4 knockout mice, ACh-induced endothelium-dependent smooth muscle relaxation (an NO-mediated effect) was also drastically reduced (14). In addition, we

Address for reprint requests and other correspondence: C. Tiruppathi, Dept. of Pharmacology (M/C 868), College of Medicine, Univ. of Illinois at Chicago, 835 S. Wolcott Ave., Chicago, IL 60612 (E-mail: tiruc@uic.edu).

The costs of publication of this article were defrayed in part by the payment of page charges. The article must therefore be hereby marked "*advertisement*" in accordance with 18 U.S.C. Section 1734 solely to indicate this fact.

showed that the increased microvascular permeability induced by PAR-1 activation was impaired in TRPC4 knockout mice (33). This finding suggests that the TRPC4-mediated Ca^{2+} influx is an important determinant of the increase in microvascular permeability. Although TRPC4 can function as SOC in mouse endothelia, recent studies have shown that expression of TRPCs in human vascular endothelial cells differs from mice (15, 25, 28, 33). However, in general, the expression profile of TRPC isoforms and their contributions in human endothelial cell signaling are not well understood.

TNF-α released during bacterial infection, such as gram-negative septicemia, contributes to the mechanism of increased microvascular permeability associated with the septicemia (8–10, 23). TNF-α also promotes increased procoagulant activity by inducing the activation of the coagulation factor thrombin (8, 9, 10, 23, 26). Recently, we showed that short-term exposure of human umbilical vein endothelial cells (HUVEC) with TNF-α augmented the thrombin-induced Ca^{2+} influx by increasing *Src* tyrosine kinase activity (36). We also showed that TNF-α increased the expression of TRPC1 by de novo protein synthesis as a result of activating the nuclear factor-κB (NF-κB) signaling pathway in HUVEC (28). This resulted in increased TRPC1 expression that in turn was associated with augmented Ca^{2+} influx after intracellular Ca^{2+} store depletion (28). Because sepsis induces both TNF-α and thrombin production, in the present study, we further addressed the relationship between TNF-α-induced expression of TRPC isoforms and the endothelial response to thrombin. We observed using RT-PCR that, in human primary endothelial cells [HUVEC and human pulmonary artery endothelial cells (HPAEC)] and the human dermal microvessel endothelial cell line [human dermal microvascular endothelial cells (HMEC)], the expression profile showed the following pattern: TRPC1 and TRPC6 expression > TRPC3 and TRPC4 > TRPC2, TRPC5, and TRPC7. TNF-α exposure selectively increased TRPC1 expression without altering the expression of other TRPC isoforms. Furthermore, the expression of TRPC1 with either TNF-α treatment or TRPC1 cDNA transfection augmented the thrombin-induced Ca^{2+} influx and endothelial barrier dysfunction. These results point to the important role of level of TRPC1 expression as being a key determinant of the endothelial permeability response.

MATERIALS AND METHODS

Materials

Human α-thrombin was obtained from Enzyme Research Laboratories (South Bend, IN). Anti-TRPC1 polyclonal antibody was raised in rabbits using hTRPC1 COOH-terminal synthetic peptide (QLYDKGYTSKEQKDC; see Ref. 40). TRIzol reagent, *Taq* DNA polymerase, LipofectAmine, LipofectAmine Plus reagent, MCDB 131, Opti-MEM I, TOPO cloning kit, and restriction enzymes were from Invitrogen (Carlsbad, CA). FuGENE 6 transfection reagent and protease inhibitor cocktail were from Roche Molecular Biochemicals (Indianapolis, IN). Fura-2 AM, Alexa-488-labeled phalloidin, and Prolong Antifade mounting medium were from Molecular Probes (Eugene, OR). PCR primers were custom synthesized from IDT (Coralville, IA). FBS was from HyClone (Logan, UT). Endothelial growth medium-2 was obtained from Cambrex Bio Science (Walkersville, MD). Human recombinant TNF-α was obtained from Alexis Biochemicals (San Diego, CA) with biological activity of 100 U/ng protein. Anti-TNF-α monoclonal antibody (mAb) was obtained from R&D Systems (Minneapolis, MN).

Methods

Cell culture. Primary culture human vascular endothelial cell types (HUVEC and HPAEC) obtained from Cambrex Bio Science were grown in endothelial cell growth medium-2 supplemented with 10% FBS. Both HUVEC and HPAEC were grown to confluence on tissue culture dishes precoated with 0.1% gelatin and were used for experiments between three and six passages. HMEC were grown in endothelial basal medium MCDB131 supplemented with 10% FBS, 10 ng/ml epidermal growth factor, 2 mM L-glutamine, and 1 μg/ml hydrocortisone (6). COS-7 cells were grown in DMEM supplemented with 10% FBS.

RT-PCR. Total RNA from HPAEC, HUVEC, and HMEC was isolated using TRIzol reagent (28). RT was performed using oligo(dT) primers and superscript RT (Invitrogen) following the manufacturer's instructions. Human TRPCs and GAPDH were amplified using the following primer sets: TRPC1 (forward, 5′-GATTTTGGAAAATTTCTTGGGATGT-3′ and reverse, 5′-TTTGTCTTCATGATTTGCTATCA-3′); TRPC2 (forward, 5′-CATCATCATGGTCATTGTGCTGC-3′ and reverse, 5′- GGTCTTGGTCAGCTCTGTGAGTC-3′), TRPC3 (forward, 5′-GACATATTCAAGTTCATGGTCCTC-3′ and reverse, 5′-ACATCACTGTCATCCTCAATTTC-3′); TRPC4 (forward, 5′-GCTTTGTTCGTGCAAATTTCC-3′ and reverse, 5′-CTGCAAATATCTCTGGGAAGA-3′); TRPC5 (forward, 5′-CAGCATTGCGTTCTGTGAAAC-3′ and reverse, 5′-CAGAGCTATCGATGAGCCTAAC-3′), TRPC6 (forward, 5′-GACATCTTCAAGTTCATGGTCATA-3′ and reverse, 5′-ATCAGCGTCATCCTCAATTTC-3′), TRPC7 (forward, 5′-CAGAAGATCGAGGACATCAGC-3′ and reverse, 3′-GTGCCGGGCATTCACGTGGTA-3′) and GAPDH (forward, 5′-TATCGTGGAAGGACTCATGACC-3′ and reverse, 5′-TACATGGCAACTGTG AGGGG-3′). RT product (2 μl) was amplified in a 50-μl volume containing 100 pmol primers and 2.5 units *Taq* DNA polymerase. Reaction conditions were as follows: 95°C for 30 s, 55°C for 30 s, 72°C for 1 min for 35 cycles, and then 72°C for 7 min. PCR products were resolved using 1.2% agarose gel and identified by ethidium bromide staining.

Quantitative RT-PCR. Relative quantitative RT-PCR was carried out to quantify the expression of TRPC1 in control and in TRPC1 cDNA-transfected HMEC. Measurement of GAPDH expression level was used to determine the exponential phase of amplification (39). For each group, a PCR master mix was prepared with normal PCR reaction components and a corresponding primer set. After 15 cycles, samples were collected out of the thermocycler. The next samples were collected with two-cycle intervals. Nine samples from *cycles 15–31* were collected for GAPDH, and 15 samples were collected between 15 and 43 cycles to determine TRPC1 transcript expression. DNA from each PCR reaction was isolated using the QIAquick PCR purification kit (Qiagen, Valencia, CA) and quantified using an ultraviolet spectrophotometer (12).

TRPC1 cDNA transfection. Human TRPC1 (hTRPC1) expression constructs were prepared as described by us (28) and transfected in HMEC using LipofectAmine Plus transfection reagent (6). We determined transfection efficiency by using green fluorescent protein expression plasmids. We observed that ~50% of HMEC were fluorescent 48 h after transfection (6). COS-7 cells were transfected with TRPC1 cDNA using FuGENE 6 transfection reagent. At 48 h after tranfection, cells were used for experiments.

Immunoblotting. Immunoblotting experiments were performed to detect both endogenous and overexpressed TRPC1 protein in HMEC. At 72 h after transfection with hTRPC1 cDNA expression construct, cells were lysed with lysis buffer (50 mM Tris·HCl, pH 7.5, 150 mM NaCl, 1 mM EGTA, 1% Triton X-100, 0.25% sodium deoxycholate, 0.1% SDS, and protease inhibitor cocktail), and the cell lysates were used for immunoblotting. Proteins were separated on SDS-PAGE and

transferred to polyvinylidene difluoride membrane strips. Nonspecific binding was blocked with 5% nonfat dry milk in TBST (10 mM Tris·HCl, pH 7.5, 0.15 M NaCl, and 0.05% Tween 20) for 1 h at 22°C and then incubated with anti-TRPC1 antibody in TBST containing 5% nonfat dry milk overnight at 4°C. After being washed with TBST, the strips were incubated with horseradish peroxidase-conjugated goat anti-rabbit secondary antibody for 1 h. The strips were washed, and the protein bands were detected by the enhanced chemiluminescence method (Amersham Biosciences).

Cytoplasmic Ca^{2+} measurement. $[Ca^{2+}]_i$ in single endothelial cells was measured by fura-2 fluorescence imaging (37). Cells grown on 25-mm-diameter glass coverslips were washed two times in Hanks' balanced salt solution (HBSS) and loaded with 3 μM fura 2-AM for 20 min at 37°C. Cells were then washed two times in HBSS and imaged by using an Attofluor RatioVision digital fluorescence microscopy system (Atto Instruments, Rockville, MD) equipped with a Zeiss Axiovert S100 inverted microscope and F-Fluar ×40, 1.3 numeric aperture oil immersion objective. Regions of interest in individual cells were marked and excited at 334 and 380 nm with emission at 520 nm at 5-s intervals. The 334- to-380-nm fluorescence ratio has been used to represent changes in $[Ca]_i$.

Patch-clamp recording of SOC current. Whole cell patch-clamp was performed on single endothelial cells adhering to glass coverlips (14). Patch electrodes were made from 1.5-mm (OD) borosilicate glass tubing. The resistance of the pipettes was ~5 MΩ when filled with internal solution (composition given below). Membrane currents were measured with a patch-clamp amplifier (Axopatch 200B; Axon Instruments, Foster City, CA) under control of pClamp 8.1 software. The currents were filtered at a corner frequency of 2 kHz with a low-pass Bessel filter and sampled at 10-ms intervals. Capacitive transients were subtracted from current records. Coverslips with cells attached were perfused at a rate of 2 ml/min; solution changes were complete within 10 s. The standard extracellular solution contained (in mM) 135 sodium glutamate, 1 $MgCl_2$, 1 $CaCl_2$, 10 glucose, and 10 HEPES buffer, pH 7.4. Internal solution contained (in mM) 135 *N*-methyl-D-glucamine, 10 CsCl, 1 BAPTA, 1 $MgCl_2$, 1 ATP, and 10 HEPES, pH 7.2 (CsOH). All experiments were performed at room temperature.

Distribution of actin stress fibers. Endothelial cells were grown to confluence on gelatin-coated glass cover slips. Cells were incubated with 1% FBS-supplemented growth medium for 2 h before exposure to thrombin (50 nM) for different time intervals. Cells were washed and fixed for 15 min with 2% paraformaldehyde in HBSS containing 10 mM HEPES buffer (pH 7.4) at 22°C and then permeabilized with 0.1% Triton X-100 for 30 min at 22°C. Cells were washed and stained with Alexa-568-labeled phalloidin for 30 min at 22°C. Cells were then washed three times with HBSS, mounted with Prolong Antifade mounting medium, and viewed through the ×60 objective of a Zeiss LSM 510 confocal microscope.

Transendothelial electrical resistance. The real-time change in endothelial monolayer resistance was measured to assess endothelial barrier function, as described by us (34). In brief, HMEC or HPAEC were grown to confluence on a small gold electrode (4.9×10^{-4} cm^2). The small electrode and the larger counter electrode were connected to a phase-sensitive lock-in amplifier. An approximate constant current of 1 μA was supplied by a 1-V, 4,000-Hz alternating current signal connected serially to a 1-MΩ resistor between the small electrode and the larger counter electrode. The voltage between the small electrode and large electrode was monitored by a lock-in amplifier, stored, and processed by a personal computer. The same computer controlled the output of the amplifier and switched the measurement to different electrodes in the course of an experiment. Before the experiment, the confluent endothelial monolayer was kept in 1% FBS-containing medium for 2 h, and then thrombin-induced change in resistance of the endothelial monolayer was measured. The data are presented in resistance normalized to its value at *time 0*, as described (7, 34). In some experiments, endothelial cells grown on the electrodes were used for transfection with TRPC1 cDNA.

Statistical analysis. Statistical comparisons were made using two-tailed Student's *t*-test. Experimental values were reported as means ± SE. Differences in mean values were considered significant at $P < 0.05$.

RESULTS

Effects of TNF-α on Expression of TRPC Homologs in Human Endothelial Cells

We have shown in recent studies that TRPC1 expression was increased in HUVEC by TNF-α exposure (28); however, it is not clear whether TNF-α also increases the expression of other TRPC isoforms in these endothelial cells. In this study, we determined expression of different TRPC isoforms in HUVEC, HPAEC, and HMEC (see *Methods* for details). We observed that TRPC1 and TRPC6 transcripts were expressed at higher levels in all three human endothelial cell types (Fig. 1*A*). The presence of TRPC3, TRPC4, and TRPC7 was detectable in these endothelial cells; however, TRPC2 and TRPC5 expression was not measurable (Fig. 1*A*).

Because all three human endothelial cell types showed a similar TRPC expression profile, we next determined the effects of TNF-α on the expression of TRPC isoforms in HPAEC. In TNF-α-stimulated HPAEC, only TRPC1 (an SOC) transcript expression increased (an increase of ~4-fold compared with control; Fig. 1*B*), whereas TRPC6 expression was unaltered (Fig. 1*B*). Exposure of TNF-α to HPAEC in the presence of neutralizing anti-TNF-α mAb prevented the TNF-α-induced TRPC1 expression (Fig. 1*B*). We did not observe any change in their expression profile of TRPC2, TRPC3, TRPC4, TRPC5, and TRPC7 isoforms in response to TNF-α compared with control (data not shown). We also determined TRPC1 protein expression in HPAEC after TNF-α challenge by immunoblot. We observed that TRPC1 protein expression was increased more than twofold at 18 h after TNF-α challenge (data not shown), which is similar to what we observed in HUVEC (28).

Because our results indicated that the TRPC1 isoform was selectively increased in TNF-α-stimulated HPAEC, we addressed the possible role of TRPC1 in the mechanism of thrombin-induced increase in $[Ca^{2+}]_i$. In the presence of extracellular Ca^{2+} (1.26 mM), thrombin produced an increase in $[Ca^{2+}]_i$ followed by a decline to baseline within 4 min after thrombin stimulation (Fig. 1*C*). In TNF-α-stimulated cells, however, the thrombin-induced increase in $[Ca^{2+}]_i$ was greatly prolonged to >8 min (Fig. 1*C*) and returned to baseline only at 15 min after thrombin stimulation. We also compared the thrombin-induced Ca^{2+} influx in control and TNF-α-stimulated cells. In this experiment, cells were first stimulated with thrombin in the absence of extracellular Ca^{2+} to deplete endoplasmic reticulum (ER) stored Ca^{2+}, and then Ca^{2+} was reapplied to assess the Ca^{2+} influx. In both control and TNF-α-treated cells, the thrombin-induced increase in the initial peak was similar; however, Ca^{2+} addition to the medium produced a twofold greater increase in Ca^{2+} influx in TNF-α-treated cells compared with control cells (Fig. 1*D*). To address the specificity of Ca^{2+} influx, we determined the effects of La^{3+} on thrombin-induced Ca^{2+} influx in both the control and

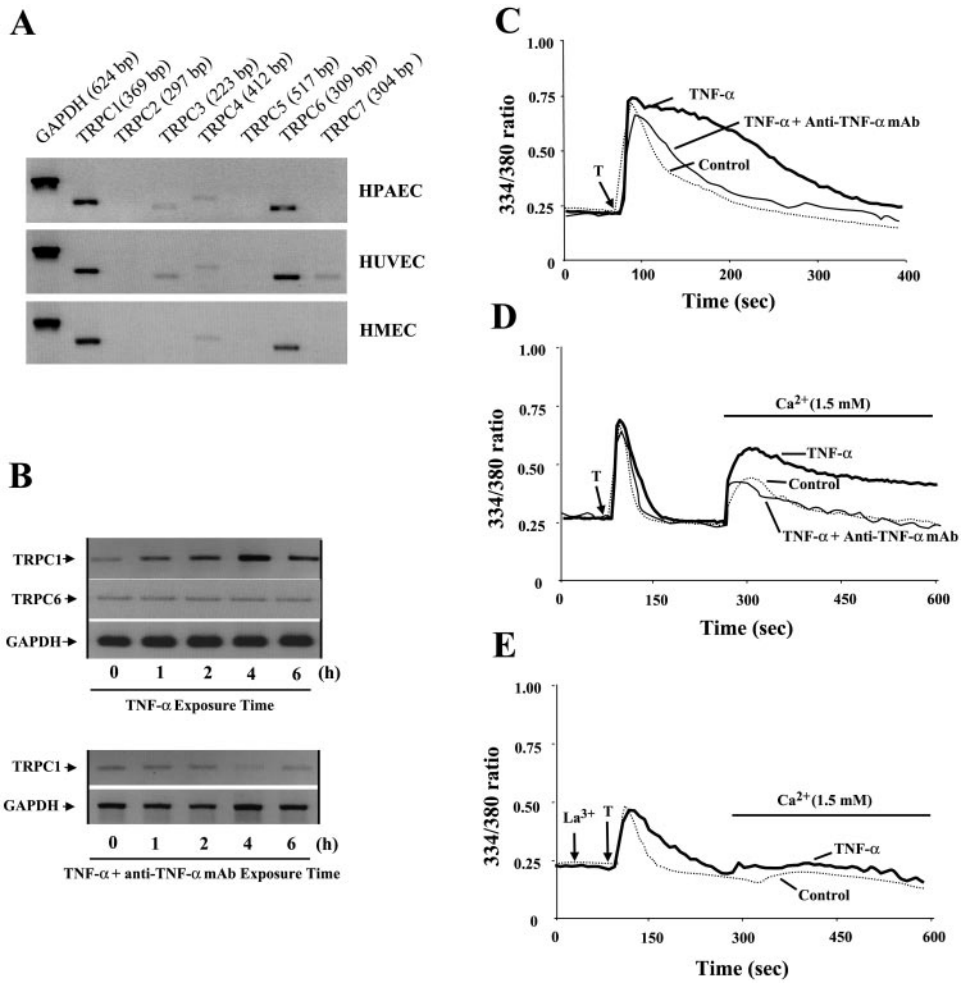

Fig. 1. *A*: expression of transient receptor potential channel (TRPC) homologues in human endothelial cells. Endogenous expression of TRPC homologues was detected by RT-PCR using total RNA isolated from human pulmonary artery endothelial cells (HPAEC), human umbilical vein endothelial cells (HUVEC), and human dermal microvascular endothelial cells (HMEC). Experimental details were described in MATERIALS AND METHODS. The expected lengths of amplified fragments were 625, 356, 297, 309, 365, 360, 309, and 304 bp for GAPDH, TRPC1, TRPC2, TRPC3, TRPC4, TRPC5, TRPC6, and TRPC7, respectively. RT-PCR profile was compared with housekeeping gene GAPDH. The experiment was repeated 3 times. *B*: TNF-α exposure increases TRPC1 expression in human endothelial cells. HPAEC were grown to confluence on gelatin-coated culture dishes. Cells were washed and incubated with 1% FBS-containing medium for 2 h at 37°C, and then cells were exposed to TNF-α (1,000 U/ml) for 0, 1, 2, 4, and 6 h. After this incubation period, total RNA was isolated using TRIzol reagent, and RT-PCR was performed to determine the mRNA expression of TRPC1, TRPC6, and GAPDH. Anti-TNF-α monoclonal antibody (mAb) prevented the TRPC1 expression. Results are representative of 4 experiments. *C–E*: TNF-α exposure augments thrombin-induced Ca^{2+} entry in HPAEC. In *C*, thrombin-induced increase in cytosolic Ca^{2+} concentration ($[Ca^{2+}]_i$) was measured in control and TNF-α-challenged cells. HPAEC grown to confluence on glass coverslips were treated with TNF-α (1,000 U/ml) for 18 h in the medium containing 1% FBS and were then loaded with 3 μM fura 2-AM for 20 min at 37°C (see MATERIALS AND METHODS for details). After fura 2-AM loading, cells were placed in nominal Ca^{2+} (1.26 mM)-containing medium and then stimulated with thrombin. Arrow indicates the time at which cells were stimulated with thrombin (25 nM). In *D*, thrombin-induced Ca^{2+} entry was measured after TNF-α exposure. HPAEC grown on glass coverslips were incubated with or without TNF-α, as described above, and then loaded with fura 2-AM for 20 min at 37°C. Cells were washed two times, placed in Ca^{2+}- and Mg^{2+}-free HBSS, and then stimulated with thrombin (25 nM). After return to baseline levels, 1.5 mM $CaCl_2$ was reapplied to the extracellular medium to induce Ca^{2+} influx. Arrows, times at which thrombin (T) or Ca^{2+} was added. In *E*, thrombin-induced Ca^{2+} influx was measured in control and TNF-α-treated cells. The experiment was carried out as described in *C* except that cells were first exposed to 100 μM $LaCl_3$ before thrombin stimulation. The results shown in *C–E* are from representative experiments. The experiments were repeated 4 times, and the data obtained were similar.

TNF-α-treated cells. La^{3+} addition did not influence the initial peak Ca^{2+} response, but Ca^{2+} entry resulting from thrombin was blocked in both the control and TNF-α-treated cells (Fig. 1*E*). We also determined the TNF-α effect in the presence of anti-TNF-α mAb and observed that the anti-TNF-α mAb prevented the TNF-α effect (Fig. 1*C*).

TRPC1 cDNA Expression Increases Store-operated Ca^{2+} Influx in Endothelial Cells

Because TRPC1 was the predominant SOC isoform expressed in human endothelial cells and its level was selectively increased in response to TNF-α stimulation, to study the

relationship between TRPC1 activation and endothelial permeability, we ectopically expressed TRPC1 in the HMEC line. To determine TRPC1 transcript copy number by relative quantitative RT-PCR, equal amounts of total RNA from the vector (pCR3.1) and TRPC1 cDNA-transfected HMEC were reverse transcribed, products were PCR amplified at different cycles, and the total amount of amplified DNA was plotted against the number of cycles to evaluate the shift in the amplification curve (Fig. 2, *A* and *B*). Relative expression levels of TRPC1 and GAPDH are shown in Fig. 2, *A* and *B*. The first detectable band of GAPDH was visible at *cycle 15* for both vector (control) and TRPC1-transfected cells (Fig. 2, *A* and *B*), remained identical, and reached a plateau after 31 cycles. In the case of TRPC1-transfected endothelial cells, the amplified DNA was detectable at *cycle 27*, whereas in control cells TRPC1 was detectable at *cycle 29* (Fig. 2, *A* and *B*). The amplification curve showed that GAPDH level was unchanged, whereas a two-cycle shift occurred in the case of TRPC1-transfected HMEC, indicating at least a fourfold increase in TRPC1 mRNA (Fig. 2*B*). We also determined TRPC1 protein expression in TRPC1 cDNA-transfected and control cells. At 72 h after transfection, cell lysates were immununoblotted with anti-TRPC1 antibody to assess TRPC1 protein expression. TRPC1 protein expression was increased approximately threefold (Fig. 2*C*) in TRPC1 cDNA-transfected HMEC compared with control (i.e., vector alone transfected).

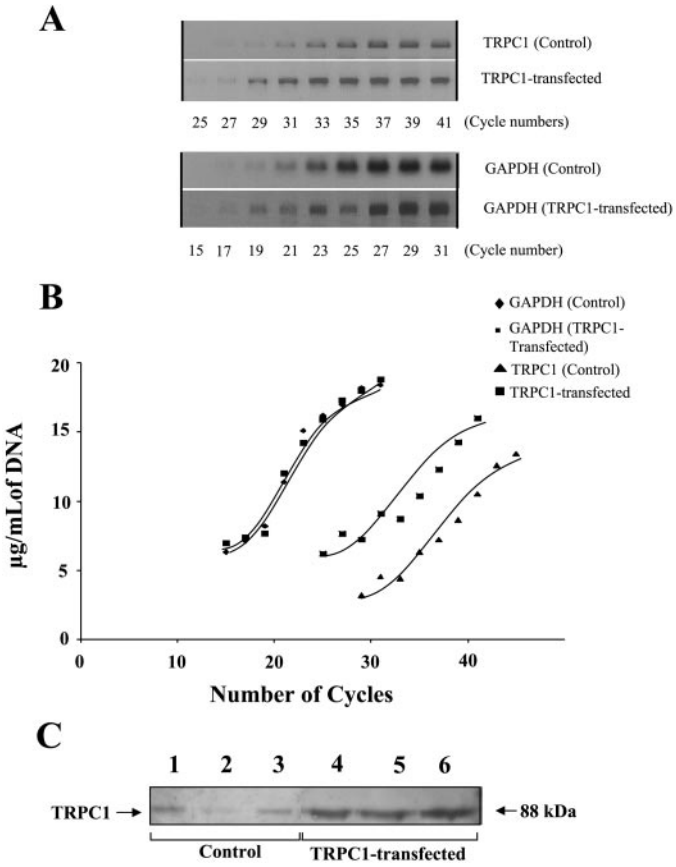

Fig. 2. *A*: TRPC1 cDNA transfection in HMEC increases TRPC1 expression. HMEC were transfected with TRPC1 cDNA using LipofectAmine plus reagent, as described in MATERIALS AND METHODS. At 72 h after transfection, total RNA was isolated, and relative quantitative RT-PCR was performed to determine the TRPC1 transcript expression. The amplification of TRPC1 and GAPDH was monitored from *cycle 15* to *cycle 41*. Amplified PCR products were resolved in 1.5% agarose gel and stained with ethidium bromide. In control HMEC, TRPC1 transcript was detectable after 29 PCR cycles, whereas in the case of HMEC transfected with TRPC1 cDNA, TRPC1 transcript was detectable after 27 PCR cycles, indicating a 4-fold increase in TRPC1 transcript in transfected HMEC. Results are representative of 4 experiments. *B*: PCR amplification curve of GAPDH and TRPC1 in control and transfected cells shows that 2 PCR cycles induce shifting of the trend line for TRPC1 cDNA-transfected HMEC compared with control HMEC. The lines for GAPDH overlap with each other, indicating no variation of transcripts. Results are representative of 4 experiments. *C*: TRPC1 cDNA transfection in HMEC increases TRPC1 protein expression. HMEC were transfected with either vector alone (pCR3.1) or TRPC1 cDNA using LipofectAmine. At 72 h after transfection, cells were lysed, and lysate (50 μg protein) was immunoblotted with anti-TRPC1 peptide antibody (Ab). This peptide Ab specifically reacted with 88-kDa protein. Anti-TRPC1 Ab reactivity was not detectable in the presence of immunogenic peptide (data not shown). *Lanes 1–3* represent samples transfected with control vector (pCR3.1), and *lanes 4–6* represent samples transfected with TRPC1 cDNA. Results are representative of 4 experiments.

We measured store Ca^{2+} depletion-mediated Ca^{2+} influx in control and TRPC1-overexpressing HMEC. In vector-transfected cells, thrombin caused a transient increase of $[Ca^{2+}]_i$ followed by a gradual decline to the basal level within 3 min (Fig. 3*A*), whereas, in TRPC1 cDNA-transfected cells, thrombin produced an initial peak increase followed by a markedly slow decline to baseline (Fig. 3*A*). Next, we measured Ca^{2+} influx in response to thrombin-induced ER stored Ca^{2+} depletion in TRPC1-transfected and control cells. In this experiment, cells were first stimulated with thrombin in the absence of extracellular Ca^{2+} to deplete ER-stored Ca^{2+}, and then Ca^{2+} was readded to assess the Ca^{2+} influx. Thrombin produced an initial peak increase in $[Ca^{2+}]_i$ that rapidly returned to the baseline value in control and TRPC1 cDNA-transfected cells (Fig. 3*B*). The addition of Ca^{2+} (1.5 mM) to the extracellular medium after thrombin-induced Ca^{2+} store depletion caused Ca^{2+} entry in both control and TRPC1-transfected HMEC (Fig. 3*B*); however, in TRPC1-transfected HMEC, Ca^{2+} influx was approximately twofold greater than control, indicating that TRPC1 expression in HMEC is responsible for the increased Ca^{2+} influx. To address the specificity of Ca^{2+} influx, we measured the effect of La^{3+} on thrombin-induced Ca^{2+} influx in control and TRPC1-transfected cells. Pretreatment of cells with 100 μM $LaCl_3$ prevented the thrombin-induced Ca^{2+} influx in both control and TRPC1-transfected cells (data not shown). Moreover, we transfeced TRPC1 antisense construct into HMEC and measured the thrombin-induced increase in $[Ca^{2+}]_i$. In TRPC1 antisense-transfected cells, Ca^{2+} influx was markedly reduced compared with control (Fig. 3*B*).

To address whether the increased TRPC1 expression has any influence on basal Ca^{2+} influx (i.e., constitutive channel activity), we measured Ca^{2+} influx in the absence of ER-stored Ca^{2+} depletion. In this experiment, fura 2-loaded cells were incubated in the absence of extracellular Ca^{2+}, and then Ca^{2+} was added back to the extracellular medium to assess Ca^{2+} entry. In TRPC1-transfected cells, Ca^{2+} entry was markedly increased compared with vector alone-transfected cells (Fig. 3*C*). Moreover, $LaCl_3$ prevented the basal Ca^{2+} influx in TRPC1-transfected cells (Fig. 3*C*), indicating that TRPC1 also regulates the constitutive Ca^{2+} influx pathway in endothelial cells.

To further address TRPC1 function, we transfected Myc-TRPC1 cDNA in COS-7 cells and measured the thapsigargin-induced increase in $[Ca^{2+}]_i$. In Myc-TRPC1-transfected cells,

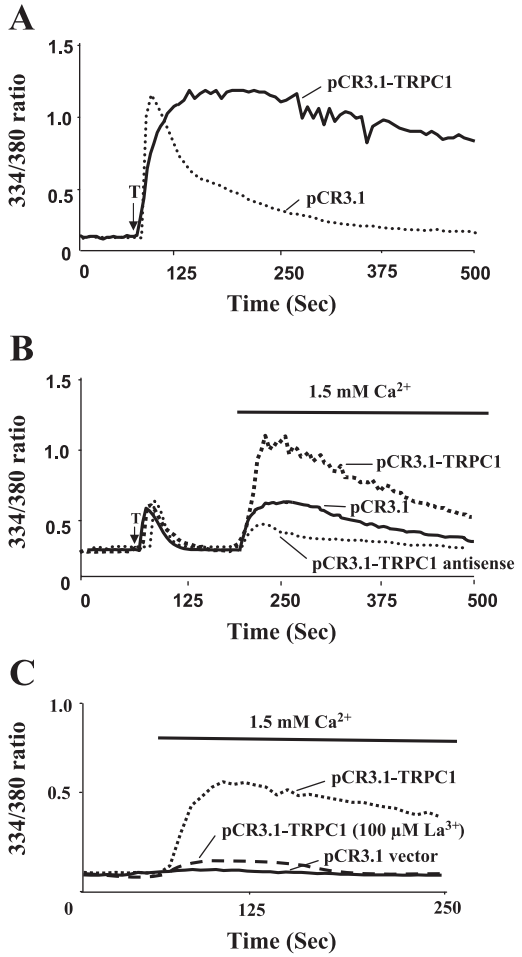

Fig. 3. *A*: overexpression of TRPC1 augments the thrombin-induced increase in intracellular calcium ($[Ca^{2+}]_i$) in HMEC. Thrombin-induced increase in $[Ca^{2+}]_i$ was measured as described in MATERIALS AND METHODS. The increase in $[Ca^{2+}]_i$ was monitored after thrombin stimulation for a period of 500 s in control and TRPC1 cDNA-transfected cells. Results are from a representative experiment. The experiment was repeated 3 times with 3 separate transfections, and the results obtained were similar. *B*: TRPC1 overexpression augments the thrombin-induced Ca^{2+} influx in endothelial cells. HMEC transfected with pCR3.1 vector alone or TRPC1 cDNA or TRPC1 antisense construct were used for experiments. Cells were washed two times, placed in Ca^{2+}-free and Mg^{2+}-free HBSS, and then stimulated with thrombin (5 U/ml). After return of $[Ca^{2+}]_i$ to the baseline level, $CaCl_2$ (1.5 mM) was added to the extracellular medium to induce Ca^{2+} influx. Results are from a representative experiment. The experiment was repeated 3 times with 3 separate transfections, and the results obtained were similar. *C*: TRPC1 overexpression augments constitutive Ca^{2+} influx in HMEC. HMEC were transfected with either vector alone or TRPC1 cDNA construct. At 72 h after transfection, cells were loaded with fura 2-AM for 30 min at 37°C. The cells were then washed two times and placed in Ca^{2+}- and Mg^{2+}-free HBSS. Ca^{2+} influx was initiated by the application of 1.5 mM $CaCl_2$ to the extracellular medium. To study the effect of La^{3+}, cells were first exposed to 100 μM $LaCl_3$, and then $CaCl_2$ was added to the extracellular medium. Results are from a representative experiment. The experiment was repeated 3 times with 3 separate transfections, and the results obtained were similar.

thapsigargin produced an approximately twofold increase in $[Ca^{2+}]_i$ compared with vector alone-transfected cells (Fig. 4*A*). In this experiment, we also measured the thapsigargin-induced Ca^{2+} influx, as described above in Fig. 3*B*. We observed an approximately twofold increase in Ca^{2+} influx in Myc-TRPC1 cDNA-transfected COS-7 cells compared with controls (Fig. 4*B*).

Relationship Between TRPC1 Expression and Store-operated Current

Because TRPC1 expression augmented Ca^{2+} influx through SOCs, we studied the magnitude of inward current on TRPC1 activation by store Ca^{2+} depletion. We presumed that cell currents (I) generated by Ca^{2+} influx through SOCs are a function of the number (N) of open TRPC1 channels and the current through the single TRPC1 channel based on the equation: $I = N \times i \times P_{open}$, where i is amplitude of single channel current and P_{open} is steady-state open probability of the channel; thus, it is predicted that, when TRPC1 channel expression is increased, the whole cell current through the channels should rise (27). To test this idea, we dialyzed HMEC with 30 μM inositol 1,4,5-trisphosphate (IP_3) through the patch pipette to open the channels. Within 2 min of patch rupture, a sustained inward current developed at −50 mV that reached a stationary level within ~1 min. The net inward current in control HMEC stimulated by IP_3 was 2.09 ± 0.18 pA/pF ($n = 5$; Fig. 5, *A-C*),

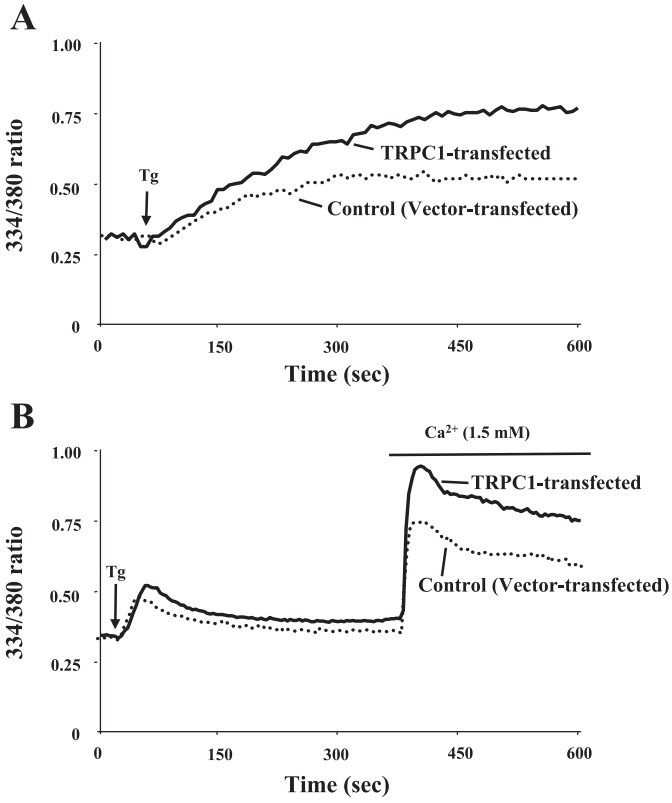

Fig. 4. TRPC1 expression in COS-7 cells increases thapsigargin (Tg)-stimulated Ca^{2+} influx. COS-7 cells grown on glass coverslips were transfected with Myc-TRPC1 cDNA (TRPC1) using FuGENE 6 transfection reagent. At 72 h after transfection, cells were loaded with 3 μM fura 2-AM for 30 min at 37°C (see details in MATERIALS AND METHODS). In *A*, after fura 2-AM loading, cells were used to measure Tg-stimulated increase in $[Ca^{2+}]_i$. During this measurement, the extracellular medium contained nominal Ca^{2+} (1.26 mM). Arrow indicates the time at which cells were stimulated with Tg (1 μM), and increase in $[Ca^{2+}]_i$ was measured in both TRPC1-transfected and control (vector-transfected) cells. In *B*, Tg-induced Ca^{2+} entry was measured. In this experiment, after cells were loaded with fura 2-AM, cells were washed two times and placed in Ca^{2+}- and Mg^{2+}-free HBSS, and then cells were stimulated with Tg (1 μM). After return of $[Ca^{2+}]_i$ to baseline levels, cells were stimulated with $CaCl_2$ (1.5 mM) to induce Ca^{2+} influx. Arrow, time at which Tg was added. Data from a representative experiment are shown. The experiment was repeated 4 times with similar results.

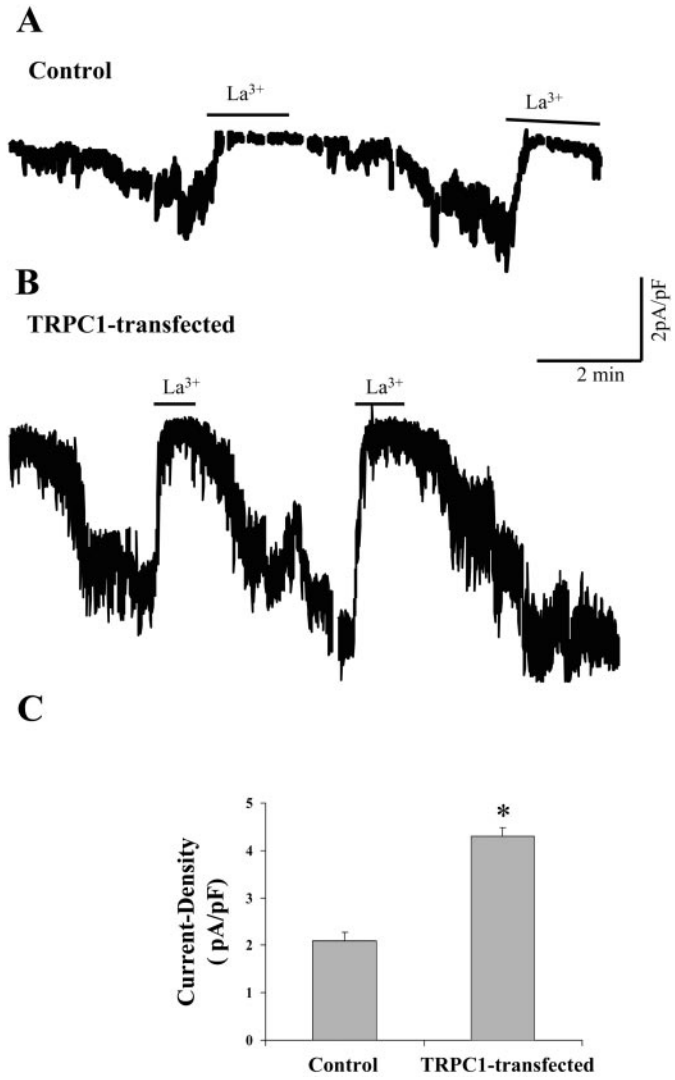

Fig. 5. Effects of increased TRPC1 expression on store-operated cationic current in HMEC. HMEC transfected with pCR3.1 (control) or pCR3.1-TRPC1 (TRPC1 transfection) were used in this experiment. Single cell was voltage-clamped to a potential of −50 mV, using a patch pipette containing inositol 1,4,5-trisphosphate plus dibenzohydroquinone to induce endoplasmic reticulum depletion. An La^{3+} (100 μM)-sensitive inward current through SOCs developed with 2–3 min of patch rupture. *A–B*: currents recorded from control HMEC (*A*) and cells with increased expression of TRPC1 (*B*). *C*: mean value of current density ($n = 6$/group) in control and transfected cells. Note inward current density greater reflecting the increased TRPC1 expression in endothelial cells. *$P < 0.05$ ($n = 6$).

whereas in TRPC1-transfected HMEC, the net inward current was 4.3 ± 0.21 pA/pF. La^{3+} (100 μM) almost completely blocked this current (Fig. 5*B*). These results demonstrate the direct relationship between TRPC1 protein expression and store-operated current in endothelial cells.

TNF-α-induced TRPC1 Expression Augments Thrombin-induced Endothelial Barrier Dysfunction

To address the relationship between increased Ca^{2+} influx via TRPC1 and endothelial permeability, we measured thrombin-induced actin-stress fiber formation and transendothelial monolayer resistance (TER) in control and TNF-α challenged HPAEC. In control cells, thrombin induced actin-stress fiber formation, and these cells returned to normal 60 min after thrombin treatment (Fig. 6*A*); however, in TNF-α-challenged cells, thrombin-induced stress fiber formation persisted for >90 min and returned to normal 2 h after thrombin stimulation (Fig. 6*A*). Next, we measured the change in TER in control and TNF-α-stimulated HPAEC. In controls, thrombin produced an ~33% decrease in TER that returned to normal within 2 h after thrombin challenge (Fig. 6, *B* and *C*), whereas in TNF-α-stimulated cells an ~55% decrease in TER was observed (Fig. 6, *B* and *C*), and the TER returned to normal 4 h after thrombin challenge (Fig. 6*B*).

We also measured thrombin-induced actin-stress formation and the decrease in TER in TRPC1-transfected HMEC and control HMEC. In control cells, thrombin increased the actin-stress fiber formation, and actin filamentous changes returned to normal within 2 h (Fig. 6*D*), whereas, in TRPC1-transfected cells, thrombin-induced actin-stress fiber showed prolonged recovery compared with control cells (Fig. 6*D*). Moreover, thrombin produced an ~30% maximum decrease in TER, and TER returned to normal within 1 h after thrombin challenge in control cells (Fig. 6, *E* and *F*). However, in TRPC1-transfected cells, thrombin produced an ~55% maximum decrease in TER, and TER returned to normal 2 h after thrombin challenge (Fig. 6, *E* and *F*).

DISCUSSION

Recent studies have shown that the members of the canonical TRPC isoform family provide the structural basis of SOCs in mammalian cells (2, 14, 27, 29, 33). Studies have also demonstrated that the pattern of expression of these TRPC isoforms differs between mouse and human endothelial cells (13, 14, 27, 33). Mouse endothelial cells express TRPC4 as the predominant isoform (14, 33), such that TRPC4 deletion [TRPC4 knockout ($TRPC4^{-/-}$)] resulted in impaired SOC-mediated Ca^{2+} influx in endothelial cells (33). In the present study, we determined the expression of TRPC isoforms in human endothelial cells. We observed that, among the seven TRPC isoforms, TRPC1 and TRPC6 were predominantly expressed in HUVEC, HPAEC, and HMEC. Interestingly, we observed that TNF-α stimulation only increased the expression of TRPC1 in these human vascular endothelial cells. The TNF-α-induced TRPC1 expression also resulted in augmentation of Ca^{2+} influx in response to store Ca^{2+} depletion. In addition, we observed that ectopic expression of TRPC1 in HMEC mimicked the TNF-α effect in amplifying the influx of Ca^{2+} after store Ca^{2+} depletion.

Acute lung injury, acute respiratory distress syndrome (ARDS), and bacterial infection-induced sepsis are clinical manifestations of lung vascular inflammation, respiratory dysfunction, polymorphonuclear neutrophil (PMN) sequestration in the lung tissue, and the accumulation of protein-rich edema fluid in the air spaces as a result of increased permeability of both the capillary and alveolar barriers (23, 41). The increased production of inflammatory cytokines, such as TNF-α and interleukin (IL)-1β, and chemokines, including IL-8 and macrophage inflammatory protein-2α from the activated macrophages and monocytes, contributes to the vascular inflammatory process (11, 41). These mediators promote PMN sequestration by increasing the expression of endothelial cell adhesion molecules via the activation of the key inflammatory

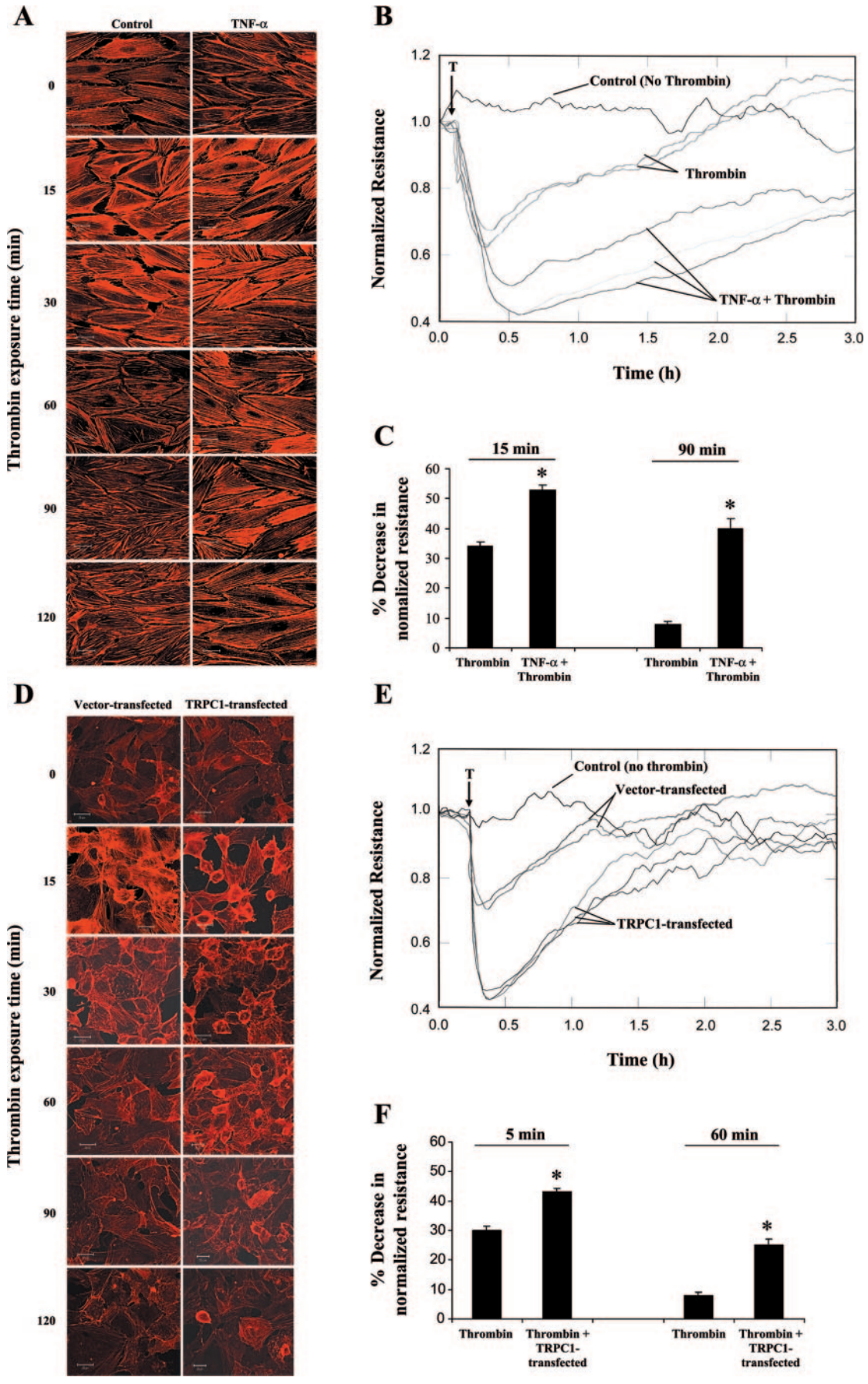
A
Control
TNF-α
Thrombin exposure time (min)
0
15
30
60
90
120
B
Normalized Resistance
T
Control (No Thrombin)
Thrombin
TNF-α + Thrombin
Time (h)
C
15 min
90 min
% Decrease in nomalized resistance
Thrombin
TNF-α + Thrombin
D
Vector-transfected
TRPC1-transfected
Thrombin exposure time (min)
E
Normalized Resistance
Control (no thrombin)
Vector-transfected
TRPC1-transfected
Time (h)
F
5 min
60 min
% Decrease in normalized resistance
Thrombin
Thrombin + TRPC1-transfected

transcription factor NF-κB in endothelial cells (11, 41). TNF-α generation in the vascular bed specifically decreases the natural anticoagulant pathways (9, 10, 23) by downregulating the expression of thrombomodulin and protein C receptor in endothelial cells, and other molecules of the coagulation system that are necessary for the conversion of inactive protein C to activated protein C (9, 10, 23). The decrease in natural anticoagulant components in the vascular bed increases thrombin generation, which can activate protease-activated receptors, such as PAR-1, on endothelial cell surface (7, 38). We have shown in a number of studies that PAR-1 activation in endothelial cells increases permeability both in vitro and ex vivo (7, 31, 33, 38). Furthermore, we showed that store-operated Ca^{2+} influx signaling is critical in the mechanism of increased endothelial permeability (33, 35). In addition, recently, we showed that the canonical cation channel TRPC1, which is an essential component of SOC in human endothelial cells, is upregulated in response to TNF-α (28). TNF-α-induced TRPC1 expression in endothelial cells occurred via the NF-κB signaling pathway (28). Therefore, it is possible that NF-κB activation-dependent TRPC1 expression in microvascular endothelial cells may contribute to the pulmonary edema associated with ARDS.

Influx of Ca^{2+} via some of the TRPC isoforms (TRPC1, TRPC4, and TRPC5) is achieved by IP_3-induced depletion of Ca^{2+} stores or preventing the Ca^{2+} refilling process by inhibiting the Ca^{2+} pump (Ca^{2+}-ATPase) using thapsigargin. Ca^{2+} influx by other TRPC isoforms (TRPC3, TRPC6) is mediated by phosphatidylinositol 4,5-bisphosphate (PIP_2) hydrolysis, likely via the involvement of IP_3, diacylglycerol, or PIP_2 (14, 17, 22). TRPC homologues can coassemble as tetramer or multimer complexes to form functional SOCs (32). Association of TRPC1 with TRPC4, or TRPC5 or TRPC1 itself was shown by coexpression and fluorescence resonance energy transfer analysis (16); however, in endothelial cells, it is unclear whether TRPC1 alone coassembles or oligomerizes with other isoforms to form functional SOCs. We have previously shown that the proinflammatory cytokine TNF-α induces TRPC1 expression in HUVEC (28). Also, the increased TRPC1 expression after TNF-α challenge was associated with augmented Ca^{2+} influx in response to ER-stored Ca^{2+} depletion (28). In the present study, we analyzed the effects of TNF-α on the expression of multiple TRPC isoforms in HPAEC. We observed that only TRPC1 expression was increased in response to TNF-α challenge. Importantly, the thrombin-induced Ca^{2+} influx was approximately twofold greater in TNF-α-stimulated cells than in control cells, indicating that TRPC1 expression is chiefly responsible for the enhanced Ca^{2+} influx.

To further address the effects of TRPC1 expression in regulating endothelial function, we also ectopically expressed TRPC1. We observed that, in TRPC1 cDNA-transfected HMEC, TRPC1 mRNA and protein levels were increased approximately fourfold and approximately threefold, respectively. We noted that the increased TRPC1 expression produced a markedly greater Ca^{2+} influx in response to ER-stored Ca^{2+} depletion. Expression of TRPC1 in COS-7 cells also showed enhanced Ca^{2+} influx when ER Ca^{2+} stores were depleted using thapsigargin. We observed additionally that the basal Ca^{2+} influx (i.e., constitutive channel activity) was increased in TRPC1-transfected HMEC compared with control cells. To address the relationship between TRPC1 expression and endothelial function, we measured IP_3-induced store-operated current in control and TRPC1 cDNA-expressing HMEC. These results showed that the IP_3-induced store-operated current was increased proportionately to the increased TRPC1 expression. Thus these results point to the role of the level of TRPC1 expression as being important in activating SOCs and mediating Ca^{2+} influx in human vascular endothelial cells.

We have shown previously that the increase in intracellular Ca^{2+} plays an essential role in signaling the increased endothelial permeability (30, 31, 33, 38). Agonists such as thrombin mediate endothelial barrier dysfunction by activating store-operated Ca^{2+} influx (30, 33). We showed that Ca^{2+} influx stimulates downstream signaling events, such as activation of myosin light chain kinase, to induce cytoskeletal reorganization, which is a prerequisite for interendothelial gap formation and the subsequent increase in endothelial permeability (35). Because we observed that TRPC1 was predominantly ex-

Fig. 6. *A*: effects of TNF-α exposure on thrombin-induced actin stress fiber formation. HPAEC were grown to confluence on gelatin-coated glass coverslips. Cells were incubated with 1,000 U/ml TNF-α for 18 h in medium containing 1% FBS and then washed and incubated with 1% FBS-containing medium for 2 h at 37°C. Cells were then challenged with thrombin (5 U/ml) for the indicated times. Cells were then washed with HBSS, fixed with 1% paraformaldehyde for 15 min at 22°C, and permeabilized with 0.1% Triton X-100 for 30 min at 22°C. Cells were stained with Alexa 568-phalloidin, washed 2 times with HBSS, mounted with ProLong antifade mounting medium, and viewed with a confocal microscope. Results are from a representative experiment. The experiment was repeated 3 times with 3 separate transfections, and the results obtained were similar. *B*: TNF-α-induced TRPC1 expression in HPAEC augments thrombin-induced decrease in transendothelial monolayer electrical resistance (TER). HPAEC were grown to confluence on gold electrode (see MATERIALS AND METHODS). Before thrombin challenge, cells were treated with or without TNF-α (1,000 U/ml) for 18 h in medium containing 1% FBS at 37°C. Cells were then challenged with thrombin (5 U/ml) to measure changes in TER. Arrow indicates the time thrombin (T) was added. Results are from a representative experiment. The experiment was repeated 6 times. *C*: data from the experiment in *B* presented as maximum decrease in TER at 15 and 90 min after thrombin stimulation. Values are means ± SE from 6 experiments. $*P < 0.05$ compared with thrombin alone-treated control cells. *D*: effects of TRPC1 overexpression on thrombin-induced actin fiber formation. HMEC grown on gelatin-coated glass coverslips were transfected with TRPC1 cDNA or vector alone. At 72 h after TRPC1 transfection, cells were washed and incubated with 1% FBS-containing medium for 2 h at 37°C. Cells were challenged with thrombin (5 U/ml) for the indicated times and stained with Alexa 568-phalloidin, as described in *A*. Results are from a representative experiment. Experiments were repeated 3 times with similar results. *E*: increased TRPC1 expression in HMEC augments thrombin-induced decrease in TER. HMEC grown on electrode wells were transfected with TRPC1 cDNA or vector alone, as described in MATERIALS AND METHODS. At 72 h after transfection, cells were washed and incubated with 1% FBS-containing medium for 2 h, and then cells were challenged with thrombin (5 U/ml). Arrow indicates the time thrombin (T) was added. Results are from a representative experiment. *F*: data from the experiment in *E* presented as a maximum decrease in TER at 5 and 60 min after thrombin stimulation. Values are means ± SE from 6 experiments. $*P < 0.05$ compared with vector-transfected cells.

pressed in human endothelial cells and TNF-α challenge only increased TRPC1 expression, we addressed the relationship between Ca^{2+} influx through TRPC1 and the increased endothelial permeability response. We exposed HPAEC to TNF-α for 18 h [the time required to induce TRPC1 expression (28)] and assessed cytoskeletal and endothelial permeability by measuring acting stress fiber formation and TER. In control cells, thrombin induced actin-stress fiber formation, and the cells returned to normal 60 min after thrombin; however, in TNF-α-challenged endothelial cells, the thrombin-induced stress fiber formation persisted for >90 min and returned to normal levels only 2 h after thrombin stimulation. Thrombin produced an ~33% decrease in TER, and this returned to normal levels within 2 h after thrombin challenge in control cells, whereas, in TNF-α-stimulated cells, the thrombin-induced decrease in TER was augmented, and the value returned to normal 4 h after thrombin challenge. We also determined actin-stress fiber formation and the decrease in TER in TRPC1 cDNA-transfected HMEC. In TRPC1 cDNA-transfected HMEC, the thrombin-induced actin-stress fiber formation and decrease in TER persisted for a prolonged time compared with control HMEC. Taken together, these results demonstrate that the level of TRPC1 expression is a key determinant of the Ca^{2+} influx via SOCs and that it plays an important role in signaling the increased endothelial permeability response.

In summary, the present study demonstrates that TRPC1 expression is selectively increased in response to TNF-α challenge of human vascular endothelial cells. We showed that increased TRPC1 expression resulted in the augmentation of store-operated Ca^{2+} influx, indicating the important role for TRPC1 as being an essential component of SOC in human endothelial cells. We further demonstrated a direct relationship between the store-operated Ca^{2+} influx through TRPC1 and the increase in endothelial permeability. These studies raise the interesting possibility that septic patients developing "leaky" vessel syndromes, such as the ARDS, may have an inappropriately elevated level of TRPC1 expression that may be capable of enhancing the store-operated Ca^{2+} influx and thereby increasing endothelial permeability.

GRANTS

This work was supported by National Institutes of Health Grants GM-58531 and P01 HL-60678.

REFERENCES

1. **Birnbaumer L, Yidirim E, and Abramowitz J.** A comparison of the genes coding for canonical TRP channels and their M, V and P relatives. *Cell Calcium* 33: 419–432, 2003.
2. **Birnbaumer L, Zhu X, Jiang M, Boulay G, Peyton M, Vannier B, Brown D, Platano D, Sadeghi H, Stefani E, and Birnbaumer M.** On the molecular basis and regulation of cellular capacitative calcium entry: roles for Trp proteins. *Proc Natl Acad Sci USA* 93: 15195–15202, 1996.
3. **Dietrich A, Mederos Y, Schnitzler M, Emmel J, Kalwa H, Hofmann T, and Gudermann T.** N-linked protein glycosylation is a major determinant for basal TRPC3 and TRPC6 channel activity. *J Biol Chem* 278: 47842–47852, 2003.
4. **Dudek SM and Garcia JG.** Cytoskeletal regulation of pulmonary vascular permeability. *J Appl Physiol* 91: 1487–1500, 2001.
5. **Dull, RO, Jaffe HA, Ge M, Ryan TJ, and Malik AB.** Pulmonary vascular endothelium and coagulation. In: *The Lung*, edited by Crystal RG, West JB, Weibel ER, and Barnes PJ. Philadelphia, PA: Lippincott-Raven, 1997, p. 653–662.
6. **Ellis CA, Malik AB, Gilchrist A, Hamm H, Sandoval, Voyno-Yaseketskaya T, and Tiruppathi C.** Thrombin induces proteinase-activated receptor-1 gene expression in endothelial cells via activation of Gi-linked ras/mitogen-activated protein kinase pathway. *J Biol Chem* 274: 13718–13727, 1999.
7. **Ellis CA, Tiruppathi C, Sandoval R, Niles WD, and Malik AB.** Time course of recovery of endothelial cell surface thrombin receptor (PAR-1) expression. *Am J Physiol Cell Physiol* 276: C38–C45, 1999.
8. **Esmon CT.** The roles of protein C and thrombomodulin in the regulation of blood coagulation. *J Biol Chem* 264: 4743–4746, 1989.
9. **Esmon CT.** Inflammation and thrombosis. *J Thromb Haemost* 1: 1343–1348, 2003.
10. **Esmon CT, Fukudome K, Mather T, Bode W, Regan LM, Stearns-Kurosawa DJ, and Kurosawa S.** Inflammation, sepsis, and coagulation. *Haematologica* 84: 254–259, 1999.
11. **Fan J, Ye R, and Malik AB.** Transcriptional mechanisms of acute lung injury. *Am J Physiol Lung Cell Mol Physiol* 281: L1037–L1050, 2001.
12. **Farazmand A, Koykul W, Peippo J, Baguma-Nibasheka M, King WA, and Basrur PK.** Sex-linked genes are not silenced in fetal bovine testes expressing X-inactive specific transcript (XIST). *J Exp Zool* 290: 327–340, 2001.
13. **Freichel M, Schweig U, Staffenberger S, Freise D, Schorb W, and Flockerzi V.** Store-operated cation channels in the heart and cells of the cardiovascular system. *Cell Physiol Biochem* 9: 270–283, 1999.
14. **Freichel M, Suh SH, Pfeifer A, Schweig U, Trost C, Weissgerber P, Biel M, Philipp S, Freise D, Droogmans G, Hofmann F, Flockerzi V, and Nilius B.** Lack of an endothelial store-operated Ca^{2+} current impairs agonist-dependent vasorelaxation in TRP4-/- mice. *Nat Cell Biol* 3: 121–127, 2001.
15. **Groschner K, Hingel S, Lintschinger B, Balzer M, Romanin C, Zhu X, and Schreibmayer W.** Trp proteins form store-operated cation channels in human vascular endothelial cells. *FEBS Lett* 437: 101–106, 1998.
16. **Hofmann T, Schaefer M, Schultz G, and Gudermann T.** Subunit composition of mammalian transient receptor potential channels in living cells. *Proc Natl Acad Sci USA* 99: 7461–7466, 2002.
17. **Kiselyov K, Xu X, Mozhayeva G, Kuo T, Pessah I, Mignery G, Zhu X, Birnbaumer L, and Muallem S.** Functional interaction between InsP3 receptors and store-operated Htrp3 channels. *Nature* 396: 478–482, 1998.
18. **Liu X, Wang W, Sing BB, Lockwich T, Jadlowiec J, O'Connel B, Wellner R, Zhu MX, and Ambudkar IS.** Trp1, a candidate protein for the store-operated Ca^{2+} influx mechanism in salivary gland cells. *J Biol Chem* 275: 3403–3411, 2000.
19. **Lo SK, Everitt J, Gu J, and Malik AB.** Tumor necrosis factor mediates experimental pulmonary edema by ICAM-1 and CD18-dependent mechanisms. *J Clin Invest* 89: 981–988, 1993.
20. **Lum H, Aschner JL, Phillips PG, Fletcher PW, and Malik AB.** Time course of thrombin-induced increase in endothelial permeability: relationship to $[Ca^{2+}]_i$ and inositol polyphosphates. *Am J Physiol Lung Cell Mol Physiol* 263: L219–L225, 1992.
21. **Lum H and Malik AB.** Regulation of vascular endothelial barrier function. *Am J Physiol Lung Cell Mol Physiol* 267: L223–L241, 1994.
22. **Ma HT, Patterson RL, van Rossum DB, Birnbaumer L, Mikoshiba K, and Gill DL.** Requirement of inositol triphosphate receptor for activation of store-operated Ca^{2+} channels. *Science* 287: 1647–1651, 2000.
23. **Matthay MA.** Severe sepsis-a new treatment with both anticoagulant and antiinflammatory properties. *N Engl J Med* 344: 759–762, 2001.
24. **Montell C, Birnbaumer L, and Flockerzi V.** The TRP channels, a remarkably functional family. *Cell* 108: 595–598, 2002.
25. **Moore TM, Brough GH, Babal P, Kelly JJ, Li M, and Stevens T.** Store-operated calcium entry promotes shape change in pulmonary endothelial cells expressing Trp1. *Am J Physiol Lung Cell Mol Physiol* 275: L574–L582, 1998.
26. **Nawroth PP and Stern DM.** Modulation of endothelial cell hemostatic properties by tumor necrosis factor. *J Exp Med* 163: 740–745, 1986.
27. **Nilius B and Droogmans G.** Ion channels and their functional role in vascular endothelium. *Physiol Rev* 81: 1415–1459, 2001.
28. **Paria BC, Malik AB, Kwiatek AM, Rahman A, May MJ, Ghosh S, and Tiruppathi C.** Tumor necrosis factor-alpha induces nuclear factor-kappaB-dependent TRPC1 expression in endothelial cells. *J Biol Chem* 278: 37195–37203, 2003.
29. **Putney JW.** TRP, inositol 1,4,5-triphophate receptors, and capacitative calcium entry. *Proc Natl Acad Sci USA* 96: 14669–14671, 1999.
30. **Sandoval R, Malik AB, Minshall RD, Kouklis P, Ellis CA, and Tiruppathi C.** Ca^{2+} signaling and PKCα activate increased endothelial permeability by disassembly of VE-cadherin junctions. *J Physiol* 533: 433–335, 2001.

31. **Sandoval R, Malik AB, Naqvi T. Mehta D, and Tiruppathi C.** Requirement of Ca^{2+} signaling in the mechanism of thrombin-induced increase in endothelial permeability. *Am J Physiol Lung Cell Mol Physiol* 280: L239–L247, 2001.
32. **Strubing C, Krapivinsky G, Krapivinsky L, and Clapham DE.** Formation of novel TRPC channels by complex subunit interactions in embryonic brain. *J Biol Chem* 278: 39014–39019, 2003.
33. **Tiruppathi C, Freichel M, Vogel SM, Paria BC, Mehta D, Flockerzi V, and Malik AB.** Impairment of store-operated Ca^{2+} entry in TRPC4$^{-/-}$ mice interferes with increase in lung microvascular permeability. *Circ Res* 91: 70–76, 2002.
34. **Tiruppathi C, Malik AB, Del Vecchio PJ, Keese CR, and Giaever I.** Electrical method for detection of endothelial cell shape change in real time: assessment of endothelial barrier function. *Proc Natl Acad Sci USA* 89: 7919–7923, 1992.
35. **Tiruppathi C, Minshall RD, Paria BC, Vogel SM, and Malik AB.** Role of Ca^{2+} signaling in the regulation of endothelial permeability. *Vascul Pharmacol* 39: 173–185, 2003.
36. **Tiruppathi C, Naqvi T, Sandoval R, Mehta D, and Malik AB.** Synergistic effects of tumor necrosis factor-α and thrombin in increasing endothelial permeability. *Am J Physiol Lung Cell Mol Physiol* 281: L958–L968, 2001.
37. **Tiruppathi C, Yan W, Sandoval R, Naqvi T, Pronin AN, Benovic JL, and Malik AB.** G protein-coupled receptor kinase-5 regulates thrombin-activated signaling in endothelial cells. *Proc Natl Acad Sci USA* 97: 7440–7445, 2000.
38. **Vogel SM, Gao X, Mehta D, Ye RD, John TA, Andrade-Gordon P, Tiruppathi C, and Malik AB.** Abrogation of thrombin-induced increase in pulmonary microvascular permeability in PAR-1 knockout mice. *Physiol Genomics* 4: 137–145, 2000.
39. **Wall SJ and Edwards DR.** Quantitative reverse transcription-polymerase chain reaction (RT-PCR): a comparison of primer-dropping, competitive and real-time RT-PCRs. *Anal Biochem* 300: 269–273, 2002.
40. **Wang W, O'Connell B, Dykeman R, Sakai T, Delporte C, Swaim W, Zhu X, Birnbaumer L, and Ambudkar IS.** Cloning of Trp1β isoform from rat brain: immunodetection and localization of the endogenous Trp1 protein. *Am J Physiol Cell Physiol* 276: C969–C979, 1999.
41. **Ware LB and Matthay MA.** The acute respiratory distress syndrome. *N Engl J Med* 342: 1334–1349, 2000.
42. **Zhu X and Birnbaumer L.** Calcium channels formed by mammalian trp homologues. *News Physiol Sci* 13: 211–271, 1998.